

NEW METHOD

## Contrast-Enhanced MRA and 3D Visualization of Pulmonary Venous Anatomy to Assist Radiofrequency Catheter Ablation<sup>#</sup>

E. P. A. Vonken,<sup>1</sup> B. K. Velthuis,<sup>1,\*</sup> F. H. Wittkamp,<sup>2</sup> B. J. Rensing,<sup>2</sup> R. Derksen,<sup>2</sup>  
and M. J. M. Cramer<sup>2</sup>

<sup>1</sup>Department of Radiology, University Medical Center Utrecht, Utrecht, The Netherlands

<sup>2</sup>Department of Cardiology, Heart-Lung Center Utrecht, Utrecht, The Netherlands

### ABSTRACT

In pulmonary vein isolation as a treatment for atrial fibrillation the proximal part of the pulmonary veins is catheterized. A protocol for preinterventional assessment of pulmonary vein anatomy was developed, based on contrast-enhanced magnetic resonance angiography (MRA) in combination with three-dimensional visualization to tailor periprocedural angiography. The results allow for assessment of the number, morphology, and location of the ostia of the pulmonary veins, as well as complicating anatomical variations, such as common trunks and aberrant courses.

### INTRODUCTION

A possible source of paroxysmal atrial fibrillation may be the arrhythmogenic properties of cardiac tissue, extending into the proximal pulmonary veins (Jais et al., 2000). Electrical isolation of the pulmonary veins from the left atrium can resolve this problem (Pappone et al., 2000; 2001). Several methods have been devised to accomplish the isolation, e.g., with cryogenic techniques and by means of laser or radiofrequency (RF) ablation (Yang et al., 2001). At the Heart-Lung Center Utrecht,

RF ablation is performed using an electrical guiding system (LocaLisa, Medtronic) (Wittkamp et al., 1999; 2002). The placement of the guiding loop catheter is performed with fluoroscopy. The anatomy and number of veins are variable; thus, individual knowledge of the location and size of the ostia is necessary in order to estimate the required catheter size. Angiography is used during the catheterization procedure. It is, however, highly contrast consuming as countercurrent flow has to be overcome. With partial retrograde filling of the vascular tree, not all relevant side-branches may be

<sup>#</sup>Part of this work was presented at the International Society for Magnetic Resonance in Medicine's 10th scientific meeting and exhibition, 2002.

\*Correspondence: B. K. Velthuis, Department of Radiology, University Medical Center Utrecht, Utrecht, The Netherlands; E-mail: bk.velthuis@azu.nl.



visualized. Furthermore, it only visualizes an ostium once it has been identified and catheterized, so unusual geometries could be overlooked.

Several imaging strategies have been used to overcome this problem. Pulmonary anatomy has been visualized using CT (Ohno et al., 2002; Lawler and Fishman, 2002; Hidvegi, 2002) and magnetic resonance imaging (MRI) (Tan et al., 2002). Spin-echo and contrast-enhanced (CE) MRA have both been utilized and described in the literature (Bongartz et al., 1998; Greil et al., 2002; Maki et al., 2001; Neimatallah et al., 1999; Pilleul and Merchant, 2000; Schoenberg et al., 1999; Takahashi et al., 2000). In this paper we present a protocol using contrast-enhanced MRA combined with three-dimensional visualization as part of a work-up for RF catheter ablation (Godart et al., 2001). We show the results of 48 patients in whom we applied the presented method prior to catheterization.

## SUBJECTS AND METHODS

From August, 2001 to May, 2002, 48 patients scheduled for ablation were imaged before the ablation procedure. The group consisted of 37 male and 11 female patients, average age  $50 \pm 8$  years (range 25–65 yr). The MRA was performed on an outpatient basis. Atrial fibrillation was present in a few patients during the examination. Most patients had paroxysmal atrial fibrillation and were in sinus rhythm. No separate informed consent was required, as it was part of the workup for their treatment.

All imaging was performed on a 1.5 T whole body scanner with high performance gradients and options for steady-state free precession (SSFP) and black-blood prepulses (ACS-NT/Intera release 7 and later 8, Philips Medical Systems, Best, The Netherlands). A four-element synergy body-wrap around coil and later a five-element, cardiac coil were used for signal reception.

The MRI protocol started with a multi-stack, SSFP survey. Parameters were TR/TE = 3.2/1.6 ms, flip-angle  $50^\circ$ , field-of-view (FOV)  $450 \times 450$  mm, matrix size  $256 \times 256$ , and 8 mm thickness without a slice-gap. In total, 20 transverse and 12 sagittal and coronal slices were acquired without cardiac triggering or breathing compensation. Next, transverse and coronal T1-TSE anatomical images were acquired, covering the heart from base to pulmonary arteries and from apex to the superior caval vein, respectively. Parameters were TR = 1 heartbeat, TE = 4.0 ms, TSE factor 17, FOV  $300 \times 240$  mm, and matrix size  $256 \times 204$  with a 0.6 partial Fourier acquisition. A black-blood double inversion preparation was used.

In the first group of patients, a two-dimensional dynamic T1-weighted series of the four-chamber view was used for timing the contrast arrival (1 image/sec). A 3-mL test bolus of dimeglumine gadopentaacetic acid (0.5 M Gd-DTPA, Magnevist, Schering) injected at 2 mL/sec was used for this purpose, with a 20 mL saline flush. The time to maximum enhancement in the left atrium was thus obtained.

In the second group of patients, fluoroscopic triggering of the three-dimensional MRA was used. A four-chamber view was dynamically acquired during injection of the whole amount of contrast. By using the four-chamber view, the contrast can be followed entering the right atrium, lung parenchyma, etc. This gives the technician ample time to correctly initiate the next scan (three-dimensional MRA), i.e., when the contrast reached the left ventricle/descending aorta. The 4-second hardware delay was used for the breath-hold command as well as to allow time for the contrast to reach maximum level in the pulmonary veins.

The three-dimensional contrast-enhanced MRA consisted of an unangulated coronal volume extending posteriorly to include the descending aorta (Neimatallah et al., 1999). Following the injection of the bolus of double-dose contrast ( $\pm 30$  cc), the volume was acquired during breath-hold in inspiration (18 sec). Imaging parameters were TR/TE = 4.0/1.2 ms, flip-angle  $40^\circ$ , slice thickness 3.0 mm, FOV  $400 \times 312$  mm, matrix  $272 \times 136$ , and 50 slices, with randomized central sampling to prevent motion artifacts due to cardiac movement. The measured resolution of  $1.5 \times 2.3 \times 3.0$  mm was reconstructed to  $0.8 \times 0.8 \times 1.5$  mm.

After acquisition the data was transferred to a workstation (Vitrea 2.2, Vital Images, Plymouth, MA) for three-dimensional analysis. The aorta and part of the pulmonary arteries were segmented out within 5 minutes. The field-of-view was restricted to the left atrium and the proximal connecting pulmonary veins. The number and size of the pulmonary veins were recorded using a three-dimensional view of the anatomy. The maximum and minimum cross-sectional diameters were measured for each vein. Distinctive features were noted, such as proximal bifurcations and an aberrant course. To visually assess the proximal geometry an endoview from the left atrium was generated.

## RESULTS

All studies were successfully completed, with one CE-MRA examination of moderate quality. This was most likely due to a difference in cardiac output between



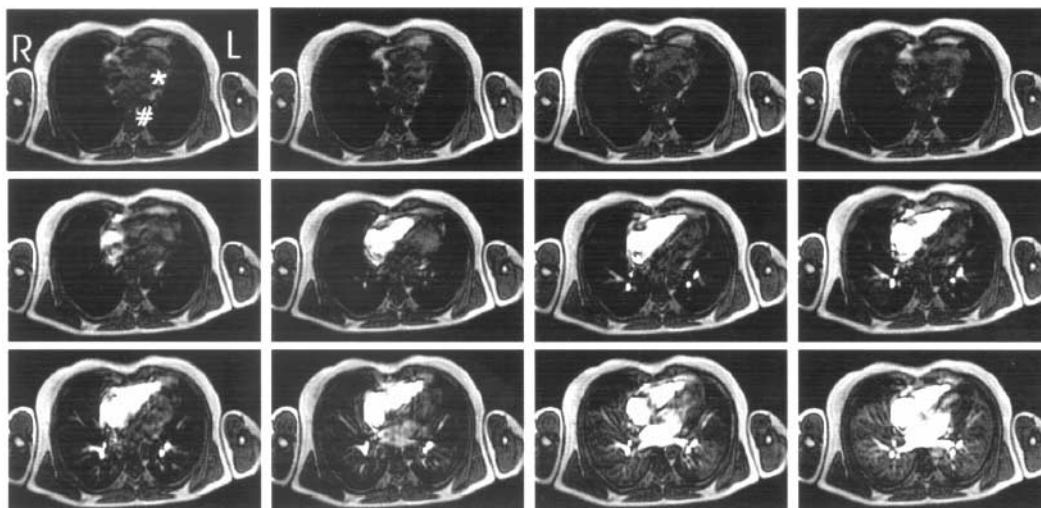


**Figure 1.** From left to right, from top to bottom: The time series used to fluoroscopically start the three-dimensional MRA (1 image/sec). The three-dimensional MRA scan is started as soon as the left ventricle (\*) or the descending aorta (#) starts enhancing.

the test and main bolus. Since the use of fluoroscopic triggering, no failures occurred (see Fig. 1).

The resulting three-dimensional images gave the cardiologists a good impression of the anatomy and sizes of the pulmonary venous ostia (see Fig. 2). The relative position of the different veins was best appreciated by interactively manipulating the viewpoint.

The most distinct shape variations observed were a common left trunk (four patients, see Fig. 3) and three pulmonary veins on the right (seven patients, see Fig. 4). Note that in two patients these features coexisted.

A summary of the average maximum and minimum sizes of different branches is shown in Table 1. A pictorial description of the geometrical variation is shown in Fig. 5.

## DISCUSSION

We have presented a protocol for visualizing the anatomy of the pulmonary veins and their branches using contrast-enhanced MRA and three-dimensional rendering. The method proved technically reliable and is well tolerated by patients.

The protocol requires about half an hour to complete the MRI examination, including patient handling, and another 25 minutes to do the postprocessing, including all measurement and endview generation. This additional time is thus added to the workup for ablation. However, isolation of the pulmonary vein ostia by catheter ablation still is a new method. In the present phase of development, the purpose of the MRA was to

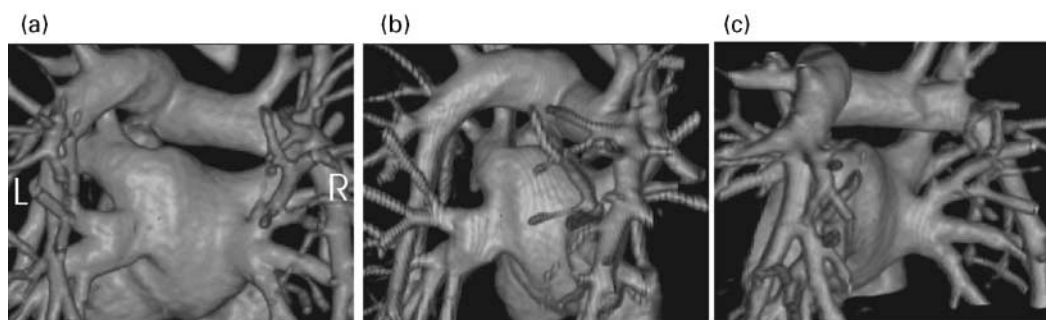


**Figure 2.** Posterior view of the left atrium (LA) of the same patient as in Fig. 1. (a) Four veins enter the LA: no aberrant coursing or distinctive sizes were observed in this patient. (b, c) Rotated view to distinguish separate veins. (*Go to [www.dekker.com](http://www.dekker.com) to view this figure in color.*)



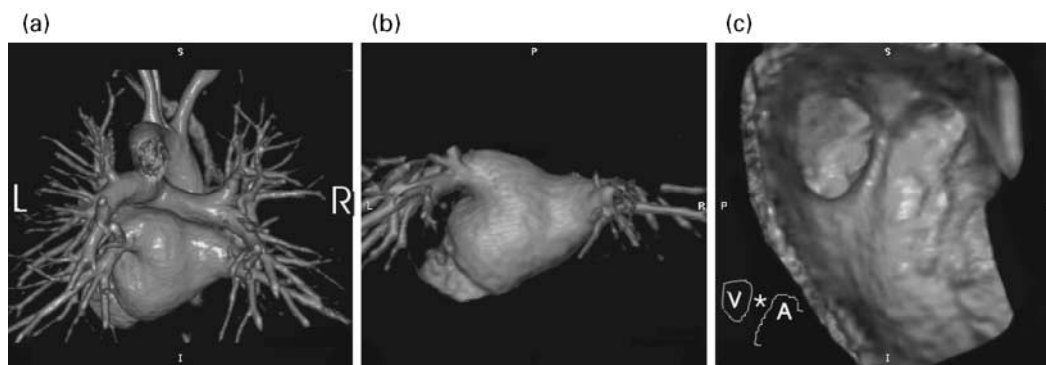


**Figure 3.** (a) Posterior view of the left atrium of a patient classified as having a single left pulmonary venous trunk. (b) Caudal view with pulmonary artery removed. (c) The wide ostium can be seen in endoview. Note the prominent ridge (\*) separating the left common vein (L) in the upper left from the left auricle (A) in the upper right of the image. (Go to [www.dekker.com](http://www.dekker.com) to view this figure in color.)

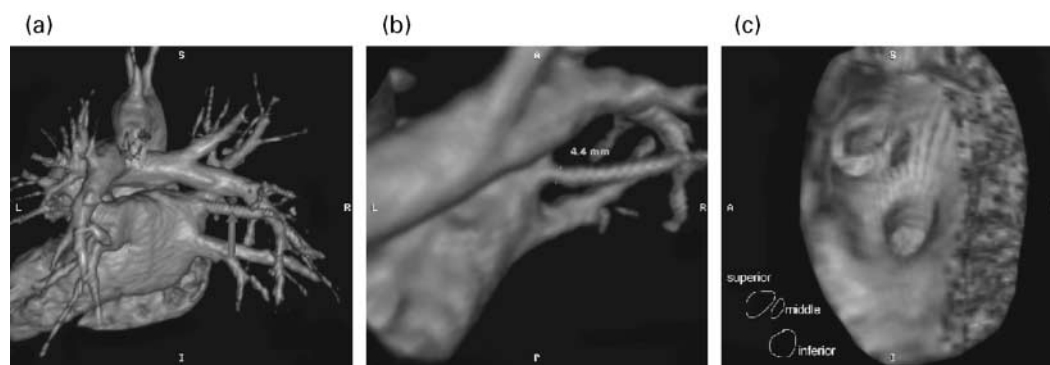


**Figure 4.** (a, b) Rendering of a patient classified as having three right pulmonary veins. (c) The endoview shows the three ostia, showing a close relationship of the superior and middle right vein entering the atrium. (Go to [www.dekker.com](http://www.dekker.com) to view this figure in color.)

focus on the quality of the catheter ablation procedure rather than on duration.

The advantage of MRA over intraprocedural angiography is the knowledge of the anatomy prior to the procedure. Prolonged searches for nonexisting pulmonary vein ostia are avoided and no relevant branches are missed. Furthermore, the gadolinium contrast agent has a

much lower complication rate and requires a smaller volume to be injected at a lower flow-rate. Of benefit is the avoidance of extra ionizing radiation, as the dose during the catheterization procedure is already substantial.

When compared with CT, MRI has the same advantages concerning radiation and contrast agent.

**Table 1.** The average, standard deviation and range of the size of the proximal pulmonary veins. The count is the number of observations in 48 patients. The maximal and minimal diameters are measured separately.

Vein	Count	Max. diameter (mm)	Min. diameter (mm)	Range (mm)
Left superior	44	18.5 ± 2.8	13.7 ± 3.7	7 ± 27
Left inferior	44	16.0 ± 3.0	11.3 ± 3.0	5 ± 23
Right superior	48	18.5 ± 3.0	15.8 ± 2.4	8 ± 25
Right inferior	48	17.7 ± 3.0	14.9 ± 2.9	9 ± 24
Right middle	7	10 ± 4	7 ± 2	3 ± 15
Left common trunk	4	27 ± 6	19 ± 7	11 ± 33

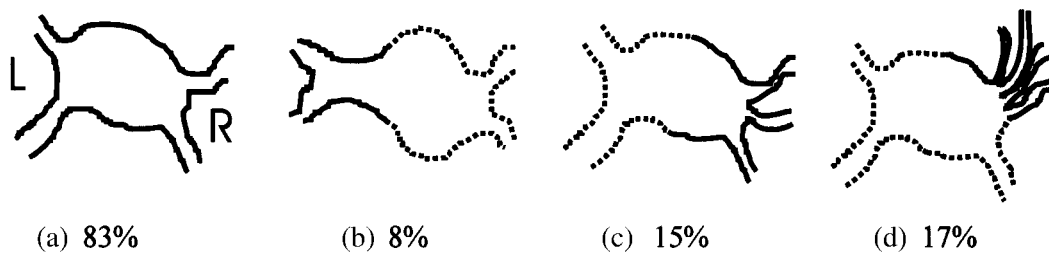


**Figure 5.** Geometrical shapes of the pulmonary venous anatomy. The relative frequency in 48 patients is shown. (a) The “normal” atrium with a superior and inferior vein draining on both the left (L) and right (R) side. (b) Variant with a common trunk on the left side. The right side is variable, with two patients having the variant of three veins. (c) Variant with three veins draining on the right side of the atrium. (d) Subvariant with one or more of the four main veins consisting of two or more vessels draining to the same ostium. This can be in combination with the more general shape as in (a), (b), and (c).

Moreover, on MRI the extra anatomical information obtained during the cardiac triggered scanning has a better soft-tissue contrast. For three-dimensional rendering, the lower contrast of CT would require more laborious segmentations. However, CT allows the simulation of the fluoroscopic image, which would require extra effort if this were desired using MRI imaging.

Moreover, CT can be used in patients who have contraindications for MRI investigation, such as claustrophobia or noncompatible implants.

Also, the spatial resolution of (multi-slice) CT is generally higher than what can be achieved with MRI in the same time-span: the acquisition is limited to the duration of a breath-hold (approximately 20 sec). The resolution of the presented MRI protocol is, however, adequate for the anatomy at hand; for reliable MRA quantification of vessel diameter, the required minimum of 3 pixels in diameter is sufficient (Frangi et al., 2001; Hany et al., 1997). The pulmonary veins are typically over 10 mm wide, thus there is limited objective benefit of a higher resolution.

The overall average size of the veins was  $16 \pm 3$  mm with a range of 5 to 27 mm. Ho et al. (2001) measured 8 to 21 mm with an average of  $13 \pm 3$  mm. Since we have no control group to evaluate these numbers in normal subjects, conclusions cannot be drawn from this observation. With respect to size, an advantage of three-dimensional visualization is the ability to measure the minimum and maximum diameter and orientation with respect to the atrium. This is contrasted to angiography, where an orientation and beam divergence dependent projection is obtained. These fundamental differences prohibit accurate determination of vessel course. Once known, two reliable orthogonal projections could be performed. With standard angiography, x-ray and contrast agent administration are required, leading to potentially deleterious side effects.

All could be done with MR without the risk of x-rays or iodinated medium contrast. We do know, however, that the average size of the ostia is in agreement with the most frequently used size of the Lasso catheter (20 mm), as the catheter has to be slightly oversized to ensure a stable position during ablation (Wittkamp et al., 2003).

The ultimate goal of imaging would be to identify the sleeves of myocardial tissue extending into the veins. However, in normal subjects, the thickness ranges from 0.05 to 1 mm proximally, and from 0.03 to 0.5 mm 10 mm into the vein (Ho et al., 2001). The resolution of the MRI imaging is currently too low to reliably identify these structures. Instead, the venous anatomy itself is measured. The classification of the anatomical variations of the pulmonary veins is somewhat subjective. When viewing the images in real-time on the workstation one gets a good impression of how the different vessels are orientated with respect to one another. When creating printouts some of the information is lost. When described in the radiology report the classification into categories is an important issue. However, no consensus exists on categorizing the sliding scale of shape variations. We used a combination of the renderings and endoview to reach a decision in classifying: When multiple vessels drained to the same area of the atrium, i.e., left or right superior or inferior, the ostium was visualized in endoview. As the different vessels appeared to be enclosed by a single (oval) ostium, it would be classified as a variant shown in Fig. 5d. When a separate ostium was seen, the Fig. 5c variant was recorded. Similarly, the existence of a common left trunk was noted. When a common space beyond the ridge separating the left pulmonary veins from the left auricle was seen, the variant of Fig. 5b was decided upon. Using this somewhat subjective method, it is interesting to notice the asymmetry of variations. No right common trunk and no three left veins were observed. A larger number of patients will be needed to



clarify the incidence of these and other variations in such patients. The description of Ho et al. (2001) is relevant.

A future development of the use of MRA might comprise the integration of the anatomical information with the non-fluoroscopic three-dimensional catheter localization techniques like Carto (BiosenseWebster) and LocaLisa (Medtronic) to provide a method of catheter navigation and guidance within the patient's three-dimensional anatomy.

### CONCLUSION

We have presented a robust method to visualize the pulmonary venous anatomy in patients with paroxysmal atrial fibrillation scheduled for RF ablation. With the extremely low toxicity of MRI contrast agent, the absence of ionizing radiation and the fast and easy segmentation of the three-dimensional datasets, the described procedure is the method of choice to assess the venous anatomy prior to the catheterization.

### ACKNOWLEDGMENTS

We gratefully acknowledge the inspiring help of P. Van Waes, professor of radiology who conceptualized the CE-MRA, as well as the assistance of N. Blanken and G. Bouwman, specialist RTs in our hospital and of E. Wever, cardiologist in the Antonius Hospital in Nieuwegein.

### REFERENCES

- Bongartz, G., Boos, M., Scheffler, K., Steinbrich, W. (1998). Pulmonary circulation. *Eur. Radiol.* 698–706.
- Frangi, A. F., Niessen, W. J., Nederkoorn, P. J., Bakker, J., Mali, W. P., Viergever, M.-A. (2001). Quantitative analysis of vascular morphology from 3D MR angiograms: in vitro and in vivo results. *Magn. Reson. Med.* 311–322.
- Godart, F., Willoteaux, S., Rey, C., Cochetoux, B., Francart, C., Beregi, J. P. (2001). Contrast enhanced magnetic resonance angiography and pulmonary venous anomalies. *Heart* 705.
- Greil, G. F., Powell, A. J., Gildein, H. P., Geva, T. (2002). Gadolinium-enhanced three-dimensional magnetic resonance angiography of pulmonary and systemic venous anomalies. *J. Am. Coll. Cardiol.* 335–341.
- Hany, T. F., Debatin, J. F., Leung, D. A., Pfammatter, T. (1997). Evaluation of the aortoiliac and renal arteries: comparison of breath-hold, contrast-enhanced, three-dimensional MR angiography with conventional catheter angiography. *Radiology* 357–362.
- Hidvegi, R. S. (2002). Anomalous single pulmonary veins. *Am. J. Roentgenol.* 507.
- Ho, S. Y., Cabrera, J. A., Tran, V. H., Farre, J., Anderson, R. H., Quintana, D. (2001). Architecture of the pulmonary veins: relevance to radio-frequency ablation. *Heart* 265–270.
- Jais, P., Shah, D. C., Haissaguerre, M., Hocini, M., Garrigue, S., Clementy, J. (2000). Atrial fibrillation: role of arrhythmogenic foci. *J. Interv. Card Electrophysiol.* 29–37.
- Lawler, L. P., Fishman, E. K. (2002). Arteriovenous malformations and systemic lung supply: evaluation by multidetector CT and three-dimensional volume rendering. *Am. J. Roentgenol.* 493–495.
- Maki, D. D., Siegelman, E. S., Roberts, D. A., Baum, R. A., Gefter, W. B. (2001). Pulmonary arteriovenous malformations: three-dimensional gadolinium-enhanced MR angiography-initial experience. *Radiology* 243–246.
- Neimatallah, M. A., Ho, V. B., Dong, Q., Williams, D., Patel, S., Song, J. H., Prince, M. R. (1999). Gadolinium-enhanced 3D magnetic resonance angiography of the thoracic vessels. *J. Magn. Reson. Imaging* 758–770.
- Ohno, Y., Hatabu, H., Takenaka, D., Adachi, S., Hirota, S., Sugimura, K. (2002). Contrast-enhanced MR perfusion imaging and MR angiography: utility for management of pulmonary arteriovenous malformations for embolotherapy. *Eur. J. Radiol.* 136–146.
- Pappone, C., Rosanio, S., Oreto, G., Tocchi, M., Gugliotta, F., Vicedomini, G., Salvati, A., Dicandia, C., Mazzone, P., Santinelli, V., Gulletta, S., Chierchia, S. (2000). Circumferential radiofrequency ablation of pulmonary vein ostia: a new anatomic approach for curing atrial fibrillation. *Circulation* 2619–2628.
- Pappone, C., Oreto, G., Rosanio, S., Vicedomini, G., Tocchi, M., Gugliotta, F., Salvati, A., Dicandia, C., Calabro, M. P., Mazzone, P., Ficarra, E., Di, G., Gulletta, S., Nardi, S., Santinelli, V., Benussi, S., Alfieri, O. (2001). Atrial electroanatomic remodeling after circumferential radiofrequency pulmonary vein ablation: efficacy of an anatomic approach in a large cohort of patients with atrial fibrillation. *Circulation* 2539–2544.



- Pilleul, F., Merchant, N. (2000). MRI of the pulmonary veins: comparison between 3D MR angiography and T1-weighted spin echo. *J. Comput. Assist. Tomogr.* 683–687.
- Schoenberg, S. O., Bock, M., Floemer, F., Grau, A., Williams, D. M., Laub, G., Knopp, M. V. (1999). High-resolution pulmonary arterio- and venography using multiple-bolus multiphase 3D-Gd-mRA. *J. Magn. Reson. Imaging* 339–346.
- Takahashi, K., Furuse, M., Hanaoka, H., Yamada, T., Mineta, M., Ono, H., Nagasawa, K., Aburano, T. (2000). Pulmonary vein and left atrial invasion by lung cancer: assessment by breath-hold gadolinium-enhanced three-dimensional MR angiography. *J. Comput. Assist. Tomogr.* 557–561.
- Tan, R. S., Behr, E. R., McKenna, W. J., Mohiaddin, R. H. (2002). Images in cardiovascular medicine. Occult anomalous pulmonary venous drainage: the clinical value of cardiac magnetic resonance imaging. *Circulation* E27–E28.
- Wittkampf, F., Loh, P., Derksen, R., Simmers, T. A., Eckardt, L. (2002). Real-time, three-dimensional, nonfluoroscopic localization of the Lasso catheter. *J. Cardiovasc. Electrophysiol.* 630.
- Wittkampf, F. H., Wever, E. F., Derksen, R., Wilde, A. A., Ramanna, H., Hauer, R. N., Robles-de-Medina, E. O. (1999). LocaLisa: new technique for real-time 3-dimensional localization of regular intracardiac electrodes. *Circulation* 1312–1317.
- Wittkampf, F. H., Vonken, E. J., Derksen, R., Loh, P., Velthuis, B., Wever, E. F., Boersma, L. V., Rensing, B. J., Cramer, M. J. (2003). Pulmonary vein ostium geometry: analysis by magnetic resonance angiography. *Circulation* 21–23.
- Yang, M., Akbari, H., Reddy, G. P., Higgins, C. B. (2001). Identification of pulmonary vein stenosis after radiofrequency ablation for atrial fibrillation using MRI. *J. Comput. Assist. Tomogr.* 34–35.

Received September 16, 2002

Accepted June 25, 2003

